Konrad-Zuse-Zentrum
für Informationstechnik Berlin

Takustraße 7
D-14195 Berlin-Dahlem
Germany

THORSTEN HOHAGE, FRANK SCHMIDT, LIN ZSCHIEDRICH

A new method for the solution of scattering problems

ZIB-Report 02-01 (Januar 2002)

A new method for the solution of scattering problems

Thorsten Hohage [*], Frank Schmidt and Lin Zschiedrich[†]
Konrad-Zuse-Zentrum Berlin

Abstract

We present a new efficient algorithm for the solution of direct time-harmonic scattering problems based on the Laplace transform. This method does not rely on an explicit knowledge of a Green function or a series representation of the solution, and it can be used for the solution of problems with radially symmetric potentials and problems with waveguides. The starting point is an alternative characterization of outgoing waves called *pole condition*, which is equivalent to Sommerfeld's radiation condition for problems with radially symmetric potentials. We obtain a new representation formula, which can be used for a numerical evaluation of the exterior field in a postprocessing step. Based on previous theoretical studies, we discuss the numerical realization of our algorithm and compare its performance to the PML method.

1 Introduction

For the solution of time-harmonic electromagnetic and acoustic scattering problems by finite element, finite difference or finite volume methods, one has to deal with a mesh termination problem: Which boundary condition has to be imposed on the artificial boundary of the computational domain such that the computed solution approximates the true solution. Such boundary conditions are called *transparent* or *absorbing*. They have to take care of the radiation condition at infinity. If the far field behavior of the solution is also of interest, one has to use a method which allows the evaluation of the solution in the exterior domain.

A variety of methods for the construction of transparent boundary conditions has been considered. The idea of *integral equation method* (cf. [3]) is to represent the solution in the exterior domain by a superposition of fundamental solutions. Another idea is to compute the *Dirichlet-to-Neumann (DtN) map* on the artificial boundary by a series representation using Hankel functions (cf. [5]). *Infinite element methods* (cf. [4]) are based on a series representation of the exterior solution, e.g. the Wilcox expansion, and use a finite element-type discretization in the exterior domain. Other authors have constructed *local approximations to the DtN-operator* of arbitrary order (cf. [8] for an overview). Finally, the *Perfectly Matched Layer (PML) Method* consists in surrounding the computational domain by a sponge layer with an anisotropic damping tensor (cf. [1, 10]).

We are particularly interested in applications in fiber optics. The simplest model of an optical fiber is an infinitely long strip in the plane with a different wave number. Under certain conditions such a strip can act as a waveguide, i.e. it can support waves which propagate without damping to infinity. In the simulation of optical components the far field behavior of the solution is of particular interest. Since for problems with an inhomogeneous exterior domain neither a fundamental solution nor a series representation of the solution is known explicitly in general, only the PML method is applicable. However, the PML method does not allow an evaluation of the solution in the exterior domain. This was one of the motivations for us to look for an alternative method.

In the following section we summarize the main ideas of our approach, and in section 3 its numerical realization. Unfortunately, our theoretical analysis in [7] only covers radially symmetric potentials, but not waveguides, yet. Therefore, in section 4 we discuss a variant of our method which requires less information about the solution, but does not allow the evaluation of the far field. As an application we present a simulation of a photonic crystal.

2 Theoretical background

We consider partial differential equations of the form

$$\Delta u(x) + (1 + p(|x|))\,\kappa^2 u(x) = 0, \qquad x \in \mathbb{R}^d, |x| > a_* \tag{1}$$

[*]supported by DFG grant number DE293/7-1; address after February 2002: University of Göttingen
[†]supported by DFG grant number SCHM 1386/1-1

with a real-valued, analytic function p of the form $p(r) = \sum_{j=2}^{\infty} p_j r^{-j}$. For $|x| \le a^*$, u may satisfy a more complicated differential equation. Let us introduce the function $U(\rho,\hat{x}) := \rho^{\frac{d-1}{2}} u(\rho\hat{x})$ defined for $\rho > a_*$, $\hat{x} \in S^{d-1}$ and its shifted Laplace transform

$$\hat{U}_a(s,\hat{x}) := \int_0^\infty e^{-sr} U(r+a,\hat{x})\,\mathrm{d}r, \tag{2}$$

for $\mathrm{Re}\, s > 0$, $\hat{x} \in S^{d-1} := \{x \in \mathbb{R}^d : |x| = 1\}$, and $a \ge a_*$. The differential equation (1) is equivalent to each of the following equations for U and $\hat{U}$:

$$\frac{\partial^2 U}{\partial \rho^2}(\rho,\hat{x}) + \frac{1}{\rho^2}(\Delta_{S^{d-1}} + C_d)U(\rho,\hat{x}) + (1+p(\rho))\,\kappa^2 U(\rho,\hat{x}) = 0, \tag{3}$$

$$(s^2+\kappa^2)\hat{U}_a(s,\hat{x}) + \int_s^\infty \left(\check{p}_a(\sigma-s) + e^{-a(\sigma-s)}(\sigma-s)(\Delta_{S^{d-1}} + C_d I)\hat{U}_a(\sigma,\hat{x})\right)\mathrm{d}\sigma = sU(a,\hat{x}) + \frac{\partial U}{\partial \rho}(a,\hat{x}). \tag{4}$$

Here $\check{p}_a(s) := e^{-as}\sum_{m=2}^{\infty} \frac{p_m}{(m-1)!} s^{m-1}$ is the inverse Laplace transform of $p(a+\cdot)$, $C_d := \frac{1}{4}(d-1)(3-d)$ and $\Delta_{S^{d-1}}$ denotes the Laplace-Beltrami operator on S^{d-1}. For $d = 1$ we set $\Delta_{S^0} := 0$. For the simplest case $p = 0$ and $d = 1$ a partial fraction decomposition yields

$$\hat{U}(s) = \frac{1}{2}\frac{U(a) - i\kappa^{-1}U'(a)}{s - i\kappa} + \frac{1}{2}\frac{U(a) + i\kappa^{-1}U'(a)}{s + i\kappa}.$$

It is easy to see that the first term is the shifted Laplace transform of the outgoing part of U given by $\frac{1}{2}(U(a) + i\kappa U'(a))e^{i\kappa(\rho-a)}$ and that the second term is the shifted Laplace transform of the incoming part. Hence, U is outgoing if and only if $\hat{U}$ does not have a pole in the lower half of the complex plane. It turns out that a similar characterization of outgoing fields is possible for $d > 1$:

Definition: (Pole Condition) *A bounded function $u : \{x \in \mathbb{R}^d : |x| > a_*\} \to \mathbb{C}$ satisfies the pole condition if for some $a \ge a_*$ the function $\hat{U}_a(\cdot,\hat{x})$ defined by (2) has a holomorphic extension to the lower complex half-plane $\mathbb{C}^- := \{s \in \mathbb{C} : \mathrm{Im}\, s < 0\}$ for all $\hat{x} \in S^{d-1}$ such that the function $s \mapsto \int_{S^{d-1}} |\frac{\partial \hat{U}_a}{\partial s}(s,\hat{x})|^2\,\mathrm{d}s(\hat{x})$ is bounded on compact subsets of $\mathbb{C}^-$.*

It is shown in [7] that a bounded solution u to the differential equation (1) satisfies the pole condition for one (and then for all!) $a \ge a_*$ if and only if it satisfies the Sommerfeld radiation condition.

In general, $\hat{U}(\cdot,\hat{x})$ does not have isolated singularities as in the example above, but singularities with a branch cuts. The most difficult part of the analysis in [7] was to show that for each Dirichlet data $U(a,\cdot)$ there exist unique Neumann data $\frac{\partial U}{\partial \rho}(a,\cdot)$ such that the integro-differential equation (4) has a solution defined on $(\mathbb{C}\backslash\{i\kappa - t : t \ge 0\}) \times S^{d-1}$. This solution has a continuous extension to the branch cut $\{i\kappa - t : t \ge 0\}$ from both sides and satisfies $|\hat{U}(s,\hat{x})| = O\big(|s|^{-1}\big)$ as $|s| \to \infty$. Moreover, the following quantities are well defined:

$$u_\infty(\hat{x}) := \lim_{s \to i\kappa} \frac{e^{-i\kappa a}\hat{U}_a(\cdot,\hat{x})}{s - i\kappa}, \tag{5}$$

$$\Psi_a(t,\hat{x}) := \frac{e^{-i\kappa a}}{2\pi i} \lim_{\varepsilon \to 0} \big(\hat{U}_a(i\kappa - t - i\varepsilon,\hat{x}) - \hat{U}_a(i\kappa - t + i\varepsilon)\big) \tag{6}$$

For an isolated pole of order 1, u_∞ denotes its residual, and Ψ_a is the jump of $\hat{U}$ across the branch cut.

If these facts have been established, we can draw some simple, but important consequences. By the Fourier inversion theorem, $U(r+a,\hat{x}) = \frac{1}{2\pi i}\int_{\varepsilon - i\infty}^{\varepsilon + i\infty} \hat{U}(s,\hat{x})e^{rs}\,\mathrm{d}s$ for any $\varepsilon > 0$. Moreover, the integral over the closed path shown in Fig. 1a) vanishes by virtue of Cauchy's integral theorem. Using the decay property of $\hat{U}$, it can be shown that the integrals over the paths γ_2^R, γ_3^R, γ_7^R, and γ_8^R vanish as $R \to \infty$. Therefore,

$$U(r+a,\hat{x}) = \frac{1}{2\pi i}\lim_{R\to\infty}\int_{\gamma_1^R} e^{rs}\hat{U}(s,\hat{x})\,\mathrm{d}s = -\frac{1}{2\pi i}\lim_{R\to\infty}\int_{\gamma_4^R+\gamma_5^R+\gamma_6^R} e^{rs}\hat{U}(s,\hat{x})\,\mathrm{d}s.$$

This yields a *representation formula* for U in terms of u_∞ and Ψ_a:

$$U(a+r,\hat{x}) = e^{i\kappa(a+r)}\left(u_\infty(\hat{x}) + \int_0^\infty e^{-tr}\Psi_a(t,\hat{x})\,\mathrm{d}t\right), \quad r \ge 0. \tag{7}$$

Note that (7) implies that u_∞ defined by (5) is the *far field pattern* or *scattering amplitude* of u.

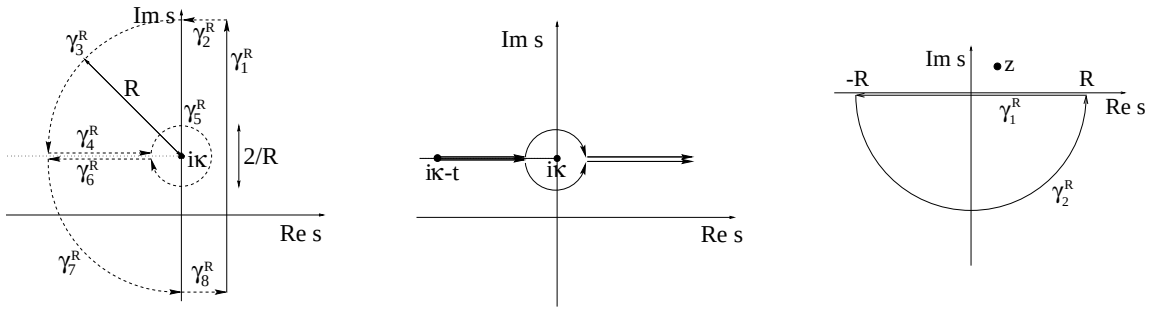

a) representation formula b) Volterra equation c) real axis approach

Figure 1: Integration paths for the proofs of the main formulas

Subtracting eq. (4) with $s = i\kappa - t + i\varepsilon$ from eq. (4) with $s = i\kappa - t - i\varepsilon$, choosing the integration paths as shown in Fig. 1b), and taking the limit $\varepsilon \to 0$ yields the Volterra integro-differential equation

$$\begin{aligned}\left\{\check{p}_a(t) + te^{-at}(\Delta_{S^{d-1}} + C_d)\right\} u_\infty(\hat{x}) + t(t-2i\kappa)\Psi_a(t,\hat{x}) \\ + \int_0^t \left\{\check{p}_a(t-t_1) + (t-t_1)e^{-a(t-t_1)}(\Delta_{S^{d-1}} + C_d I)\right\} \Psi_a(t_1,\hat{x})\,\mathrm{d}t_1 = 0.\end{aligned} \tag{8}$$

3 The cut function approach

Discretization. For simplicity we will only consider the Helmholtz equation, i.e. the case $p = 0$ although the algorithm in this section also works for $p \neq 0$. We start with the exterior Dirichlet problem on the artificial boundary $\Gamma_a := \{x : |x| = a\}$ with boundary data $f \in H^{1/2}(\Gamma_a)$:

$$\Delta u + \kappa^2 u = 0, \qquad \text{in } \{x : |x| > a\}, \tag{9a}$$

$$u = f, \qquad \text{on } \Gamma_a, \tag{9b}$$

$$u \text{ satisfies the pole condition.} \tag{9c}$$

Eq. (7) with $r = 0$ and (8) yields the following system of equations for the two unknown functions Ψ_a and u_∞

$$u_\infty(\hat{x}) + \int_0^\infty \Psi_a(t,\hat{x})\,\mathrm{d}t = e^{-i\kappa a} a^{(d-1)/2} f(\hat{x}), \tag{10a}$$

$$te^{-at}(\Delta_{S^{d-1}} + C_d I)u_\infty(\hat{x}) + t(t-2i\kappa)\Psi_a(t,\hat{x}) + \int_0^t (t-t_1)e^{-a(t-t_1)}(\Delta_{S^{d-1}} + C_d I)\Psi_a(t_1,\hat{x})\,\mathrm{d}t_1 = 0. \tag{10b}$$

We first discretize this system of equations with respect to the angular variable $\hat{x}$. This corresponds to the method of lines for evolution problems. Given a finite element mesh on S^{d-1}, let M denote the boundary mass matrix, and K the boundary stiffness matrix. Then (10) is approximated by

$$M\underline{u_\infty} + M\int_0^\infty \underline{\psi}(t)\,\mathrm{d}t = Ma^{(d-1)/2} e^{-i\kappa a}\underline{f}, \tag{11a}$$

$$(C_d M + K)\frac{\exp(-at)}{t-2i\kappa}\underline{u_\infty} + M\underline{\psi}(t) + \int_0^t \ker(t,t_1)\underline{\psi}(t_1)\,\mathrm{d}t_1 = 0, \tag{11b}$$

where the kernel is given by $\ker(t,t_1) := (K + C_d M)(t-t_1)\frac{\exp(-a(t-t_1))}{t(t-2i\kappa)}$.

The Volterra equation (11b) is solved by an extended Volterra-Runge-Kutta method (cf. Brunner and van der Houwen [2]). We choose a Runge-Kutta method represented by the Butcher scheme

$$\begin{array}{c|ccc} c_1 & a_{11} & \dots & a_{1p} \\ \vdots & \vdots & & \vdots \\ c_p & a_{p1} & \dots & a_{pp} \\ \hline & b_1 & \dots & b_p \end{array}.$$

This induces a quadrature rule $\int_0^1 \varphi(x)\,dx \approx \sum_{\nu=1}^p b_\nu \varphi(c_\nu)$ which is used for the numerical integration. Given a step sequence $0 = t_1 < t_2 < \cdots < t_{N+1}$, and the intermediate points $t_{n\nu} := t_n + c_\nu(t_{n+1} - t_n)$ for $n = 1,\ldots,N$ and $\nu = 1,\ldots,p$, we approximate (11a) by

$$M\underline{u_\infty} + \sum_{n=1}^{N}\sum_{p=1}^{\nu} w_{n\nu}\underline{\psi_{n\nu}} = Ma^{(d-1)/2}e^{-i\kappa a}\underline{f}. \tag{12}$$

Here $w_{n\nu} := (t_{n+1} - t_n)b_\nu$ and $\underline{\psi_{n\nu}} \approx \underline{\psi}(t_{n\nu})$. Eq. (11b) is approximated by

$$(C_d M + K)\frac{\exp(-at_{n\nu})}{t_{n\nu} - 2i\kappa}\underline{u_\infty} + M\underline{\psi_{n\nu}} + \sum_{\mu=1}^{p}(t_{n+1} - t_n)a_{\nu\mu}\ker(t_{n\nu}, t_{n\mu})\underline{\psi_{n\mu}} + \sum_{m=1}^{n-1}\sum_{\mu=1}^{p} w_{m\mu}\ker(t_{n\nu}, t_{m\mu})\underline{\psi_{m\mu}} = 0, \tag{13}$$

$n = 1,\ldots,N$, $\nu = 1,\ldots,p$.

Coupling to the interior problem. Usually the exterior problem (9) is coupled to an interior problem, say $\Delta u_{\rm int} + \kappa^2 u_{\rm int} = 0$ in a domain $\Omega := B_a \backslash K$ with a Neumann condition on the smooth boundary of the obstacle K contained in the ball $B_a := \{x \in \mathbb{R}^d : |x| < a\}$. Green's formula yields the weak form

$$\int_\Omega \left(\nabla u_{\rm int}\nabla\overline{v} - \kappa^2 u_{\rm int}\overline{v}\right)\,dx + \int_{\Gamma_a} \frac{\partial u_{\rm int}}{\partial n}\overline{v}\,ds = F(\overline{v}), \qquad v \in H^1(\Omega) \tag{14}$$

where $F : H^1(\Omega) \to \mathbb{C}$ is a bounded linear functional. Another equation involving the Neumann data $\frac{\partial u}{\partial n} = \frac{\partial u_{\rm int}}{\partial n}$ is obtained by differentiating (8) with respect to t:

$$i\kappa u_\infty + \int_0^\infty (i\kappa - t)\Psi_a(t)\,dt = a^{(d-1)/2}e^{-i\kappa a}\frac{\partial u}{\partial n} + \frac{d-1}{2}a^{(d-3)/2}e^{-i\kappa a} f. \tag{15}$$

We set $f = \mathrm{Tr}_{\Gamma_a} u_{\rm int}$ and write the equations (14), (10a), (10b) and (15) for the case $d = 2$ in matrix form:

$$\begin{pmatrix} \int_\Omega(-\nabla\ldots\nabla\overline{v} + \kappa^2\ldots\overline{v})\,dx & & & \int_{\Gamma_a}\ldots\overline{v}\,ds \\ -e^{-i\kappa a}\sqrt{a}\,\mathrm{Tr}_{\Gamma_a} & I & \int_0^\infty\ldots\,dt & \\ & \frac{e^{-at}}{t-2i\kappa}A & I + \int_0^t \frac{(t-t_1)e^{-a(t-t_1)}}{t(t-2i\kappa)}A\ldots\,dt_1 & \\ -\frac{e^{-i\kappa a}}{2\sqrt{a}}\,\mathrm{Tr}_{\Gamma_a} & i\kappa I & \int_0^\infty(i\kappa - t)\ldots\,dt & -e^{-i\kappa a}\sqrt{a}I \end{pmatrix} \begin{pmatrix} u_{\rm int} \\ u_\infty \\ \Psi_a \\ \frac{\partial u}{\partial n} \end{pmatrix} = \begin{pmatrix} F(\overline{v}) \\ 0 \\ 0 \\ 0 \end{pmatrix}$$

Here $A := \Delta_{S^1} - \frac{1}{4}I$. Eq. (14) is discretized by finite element technology. Eq. (15) is approximated the same way as eq. (10a).

Numerical results. The kite-shaped domain shown in Fig. 2 is a well known test example in scattering theory. We imposed the Dirichlet boundary condition $u = -u_i$ on the boundary of the kite with the incident wave $u_i(x) = e^{ix_1}$ and $\kappa = 1$. A reference solution of high accuracy was computed by the integral equation method (cf. [3]). It has been shown in [7] the $|\Psi_a(t,\hat{x})|$ decays exponentially as $t \to \infty$. This is a heuristic explanation for the experimental observation that the error in $u_{\rm int}$ and u_∞ introduced by replacing $\int_0^\infty$ by $\int_0^R$ in (10a) and (15) decays exponentially as $R \to \infty$. A rigorous proof of this observation remains an open problem. For the PML method, exponential convergence with increasing thickness of the sponge layer has been established for $p = 0$ by Lassas and Somersalo [10] using integral equation techniques. Their proof was generalized by the authors to the case $p \neq 0$ using pole condition techniques (cf.[6]).

It is advantageous to work with a non-uniform grid on the branch cut which is finer near the singularity. We have chosen $t_j = C_{\rm mesh}(j/N)^2 \ln_2 N$, $j = 0,\ldots,N$. The term $\ln_2 N$ is motivated by the exponential decay of Ψ_a. In the computations documented in Table 1 we used the Butcher schemes of the Lobatto A methods of order 4 and 6 with $C_{\rm mesh} = 1$ and $C_{\rm mesh} = 1.5$, respectively. The total number of degrees of freedom for the discretization of each component of $\underline{\Psi}_a(t)$ and u_∞ is given by $DOF = 2 + 2N$ for Lobatto 4A scheme and by $DOF = 2 + 3N$ for Lobatto 6A scheme. In Table 1 $E(\partial_r u)$ and $E(u_\infty)$ denote the relative L^2-errors in the Neumann data and the far field pattern. The results show that good accuracy can be achieved with a quite small number of degrees of freedom. This number is comparable to that of the PML method with a small difference in favor of the PML method. However, with the cut function approach we also compute the far field pattern and we can evaluate the exterior field using the representation formula (7).

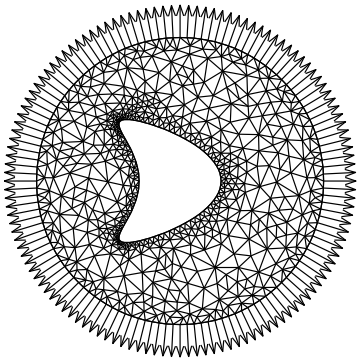

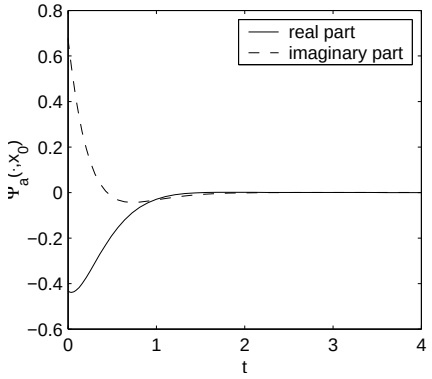

Figure 2: Finite element mesh and cut function on one of the rays

Lobatto 4A				Lobatto 6A				PML			
N	DOF	$E(\partial_r u)$	$E(u_\infty)$	N	DOF	$E(\partial_r u)$	$E(u_\infty)$	N	DOF	$E(\partial_r u)$	
4	10	3.4e-3	2.0e-3	4	13	8.0e-4	5.9e-5	4	10	1.3e-3	
8	17	4.1e-4	2.5e-4	8	26	6.4e-5	3.5e-6	8	17	2.2e-4	
16	34	8.6e-5	3.7e-5	16	50	4.3e-6	1.5e-7	16	33	1.4e-5	
32	66	1.8e-5	2.5e-6	32	98	3.5e-7	7.4 e-9	32	65	1.5e-6	

Table 1: Numerical results

4 The real axis approach

For problems with waveguides it is usually still possible to introduce a coordinate system such that the Helmholtz equation can be Laplace transformed analytically in radial direction. However, we do not know the type and the location of the singularities of $\hat{U}$ for this case, yet. In the direction of the waveguide we expect singularities at $i\beta_1, \ldots, i\beta_N$ where β_j are the propagation constants of the guided modes. To obtain a numerical solution of these problems, we compute the Laplace transform $\hat{U}$ on the real axis using eq. (4). Consider the integration path in Fig. 1c). If $\hat{U}$ satisfies the pole condition, then Cauchy's integral theorem implies that $\int_{\gamma_1^R+\gamma_2^R} \frac{\hat{U}(s,\hat{x})}{s-z}\,\mathrm{d}s = 0$ for any $z \in \mathbb{C}$ with $\mathrm{Im}\, z > 0$. Since $\hat{U}(s,\hat{x}) = O\big(|s|^{-1}\big)$ for $|s| \to \infty$, it follows that $\lim_{R\to\infty} \int_{\gamma_2^R} \frac{\hat{U}(s,\hat{x})}{s-z}\,\mathrm{d}s = 0$. Therefore,

$$\int_{\infty}^{-\infty} \frac{\hat{U}(s,\hat{x})}{s-z}\,\mathrm{d}s = 0. \tag{16}$$

We do not use the scaling factor $\rho^{(d-1)/2}$ in the definition of U in this case since the solution may behave differently for different directions. A general method of lines type discretization of the Helmholtz equation, which is appropriate for problems involving waveguides, is derived in [11].

The real axis approach has the advantage that it does not require the knowledge of the type and location of the singularities of the Laplace transform. On the other hand, it is not possible to evaluate the far field with this approach since the singularities of the Laplace transform determine the far field behavior of the solution.

In our test example (cf. Fig. 3) light enters a photonic crystal through a waveguide at the left. Photonic crystals are materials with a dielectric constant varying periodically at a length scale comparable to the wavelength of light. This can create a range of 'forbidden' frequencies called a photonic bandgap. Photons with energies lying in the bandgap cannot propagate through the medium in any direction. Recently, photonic crystals have received considerable attention of engineers, physicists, and mathematicians (cf. the review article [9] and the literature therein). One of the reasons for this popularity is that photonic crystals can mould the flow of light at a very small scale. In Fig. 3 light cannot penetrate into the areas with the periodically arranged circles. Therefore, it follows the path without circles and leaves the photonic crystal at the top.

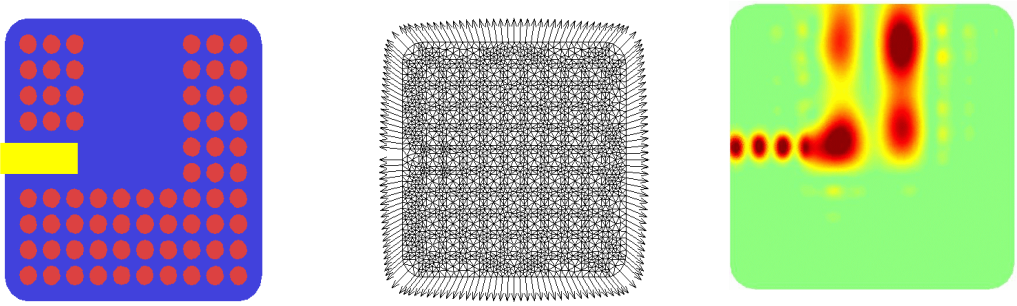

refractive index profile mesh computed solution

Figure 3: Photonic crystal

5 Conclusion

We have discussed a new method for the solution of time-harmonic scattering problems with inhomogeneous exterior domains, which is based on the Laplace transform. For the homogeneous Helmholtz equation and for radially symmetric potentials our method allows the evaluation of the exterior field and the far field pattern. For waveguide problems we have discussed a modified version of our method which only yields the solution on the computational domain.

References

[1] J. P. Bérenger. A perfectly matched layer for the absorbtion of electromagnetic waves. *J. Comput. Phys.*, 114:185–200, 1994.

[2] H. Brunner and P. J. van der Houwen. *The numerical solution of Volterra equations*, volume 3 of *CWI Monograph*. North-Holland, Amsterdam, 1986.

[3] D. Colton and R. Kreß. *Inverse Acoustic and Electromagnetic Scattering*. Springer Verlag, Berlin Heidelberg New York, second edition, 1997.

[4] L. Demkowicz and K. Gerdes. Convergence of the infinite element methods for the Helmholtz equation in separable domains. *Numer. Math.*, 79:11–42, 1998.

[5] D. Givoli. *Numerical Methods for Problems in Infinite Domains*. Number 33 in Studies in Applied Mechanics. Elsevier, Amsterdam, 1992.

[6] T. Hohage, F. Schmidt, and L. Zschiedrich. Solving time-harmonic scattering problems based on the pole condition: Convergence of the PML method. Technical Report 01-23, Konrad-Zuse-Zentrum, Berlin, 2001.

[7] T. Hohage, F. Schmidt, and L. Zschiedrich. Solving time-harmonic scattering problems based on the pole condition: Theory. Technical Report 01-01, Konrad-Zuse-Zentrum, Berlin, 2001.

[8] F. Ihlenburg. *Finite Element Analysis of Acoustic Scattering*. Springer Verlag, 1998.

[9] P. R. V. J D Joannopoulos and S. Fan. Photonic crystals: putting a new twist on light. *Nature*, 386:143–149, 1997.

[10] M. Lassas and E. Somersalo. On the existence and convergence of the solution of PML equations. *Computing*, 60:228–241, 1998.

[11] F. Schmidt. Solution of interior-extrior Helmholtz-type problems based on the pole condition: Theory and algorithms. Habilitation thesis, submitted, 2001.